Molecular Biology of the Cell
Vol. 21, 186–197, January 1, 2010

Actin-binding Protein-1 Interacts with WASp-interacting Protein to Regulate Growth Factor-induced Dorsal Ruffle Formation

Christa L. Cortesio,*† Benjamin J. Perrin,† David A. Bennin,† and Anna Huttenlocher†

Departments of *Biomolecular Chemistry, †Medical Microbiology and Immunology, and Pediatrics, University of Wisconsin, Madison, WI 53706

Submitted February 4, 2009; Revised October 28, 2009; Accepted October 29, 2009
Monitoring Editor: Josephine C. Adams

Growth factor stimulation induces the formation of dynamic actin structures known as dorsal ruffles. Mammalian actin-binding protein-1 (mAbp1) is an actin-binding protein that has been implicated in regulating clathrin-mediated endocytosis; however, a role for mAbp1 in regulating the dynamics of growth factor–induced actin-based structures has not been defined. Here we show that mAbp1 localizes to dorsal ruffles and is necessary for platelet-derived growth factor (PDGF)-mediated dorsal ruffle formation. Despite their structural similarity, we find that mAbp1 and cortactin have nonredundant functions in the regulation of dorsal ruffle formation. mAbp1, like cortactin, is a calpain 2 substrate and the preferred cleavage site occurs between the actin-binding domain and the proline-rich region, generating a C-terminal mAbp1 fragment that inhibits dorsal ruffle formation. Furthermore, mAbp1 directly interacts with the actin regulatory protein WASp-interacting protein (WIP) through its SH3 domain. Finally, we demonstrate that the interaction between mAbp1 and WIP is important in regulating dorsal ruffle formation and that WIP-mediated effects on dorsal ruffle formation require mAbp1. Taken together, these findings identify a novel role for mAbp1 in growth factor–induced dorsal ruffle formation through its interaction with WIP.

INTRODUCTION

The dynamic regulation of the actin cytoskeleton is important for many cellular processes including endocytosis, vesicle trafficking, and cell motility. The actin cytoskeleton is regulated temporally and spatially to form specialized structures such as growth factor–induced dorsal ruffles and lamellipodia. Dorsal ruffles are highly dynamic structures that form on the dorsal surface of fibroblasts and epithelial cells in response to treatment with platelet-derived growth factor (PDGF) or epidermal growth factor (EGF; Orth *et al.*, 2006; Orth and McNiven, 2006). Dorsal ruffles are important for diverse cellular processes including cell invasion (Suetsugu *et al.*, 2003) and internalization of growth factor receptors (Orth *et al.*, 2006). Several actin regulatory and binding proteins including N-WASP (Legg *et al.*, 2007), WASp-interacting protein (WIP; Anton *et al.*, 2003) and cortactin (Krueger *et al.*, 2003) localize to these structures and have been implicated in their function.

Mammalian actin-binding protein 1 (mAbp1) is an F-actin–binding protein that regulates both endocytosis and synaptic vesicle recycling (Kessels *et al.*, 2000, 2001; Connert *et al.*, 2006). mAbp1 was originally identified as a protein tyrosine kinase substrate. The N-terminal region of mAbp1 consists of an actin-depolymerizing factor homology (ADF-H) domain, followed by a charged α-helical domain, both of which bind to F-actin. After the F-actin–binding domains, there is a proline-rich region, which contains putative SH3-domain binding sites and two YXXP consensus tyrosine phosphorylation sites (Larbolette *et al.*, 1999; Kessels *et al.*, 2000). The C-terminus also contains an SH3 domain, which binds to proteins involved in endocytosis, such as dynamin 1, and signaling proteins including c-Jun N-terminal kinase (c-JNK) and the Cdc42 exchange factor Fgd1 (Kessels *et al.*, 2000; Schafer *et al.*, 2002; Fenster *et al.*, 2003; Hou *et al.*, 2003).

Previous studies have revealed regulatory roles for mAbp1 in receptor-mediated endocytosis (Kessels *et al.*, 2001; Mise-Omata *et al.*, 2003), T-cell receptor signaling and internalization, B-cell receptor antigen processing and presentation, and neutrophil adhesion and integrin-mediated phagocytosis (Le Bras *et al.*, 2004; Han *et al.*, 2005; Onabajo *et al.*, 2008; Schymeinsky *et al.*, 2009). Furthermore, mAbp1 knockout mice display severe behavioral abnormalities attributed at least in part to a defect in vesicle fusion and trafficking in neurons (Connert *et al.*, 2006). However, despite its importance in regulating endocytosis, previous studies have not investigated a role for mAbp1 in regulating actin-based structures such as dorsal ruffles.

Cortactin is another F-actin–binding protein that is structurally similar to mAbp1. It has been reported that cortactin localizes to dorsal ruffles and is necessary for dorsal ruffle formation through its interaction with dynamin (Krueger *et al.*, 2003). Cortactin contains similar domains to mAbp1 including an actin-binding domain, a proline-rich domain, and a C-terminal SH3 domain that mediates protein–protein

This article was published online ahead of print in *MBC in Press* (http://www.molbiolcell.org/cgi/doi/10.1091/mbc.E09–02–0106) on November 12, 2009.

Address correspondence to: Anna Huttenlocher (huttenlocher@wisc.edu).

Abbreviations used: mAbp1, mammalian actin-binding protein-1; N-WASP, neuronal Wiskott-Aldrich syndrome protein; PDGF, platelet-derived growth factor; WIP, Wasp-interacting protein.

interactions (Wu and Parsons, 1993; Kessels *et al.*, 2000). Cortactin activity is regulated in part by limited proteolysis mediated by the calcium-dependent protease calpain 2, and this proteolytic event has been shown to modulate both cell protrusion (Perrin *et al.*, 2006) and invadopodia dynamics (Cortesio *et al.*, 2008).

In this study we examined the role of mAbp1 in PDGF-induced dorsal ruffle formation. We show that both mAbp1 and cortactin are necessary for dorsal ruffle formation; however, despite their structural similarity, mAbp1 and cortactin have nonredundant functions in the regulation of dorsal ruffles. We identify mAbp1 as a novel calpain 2 substrate and show that a cleavage fragment of mAbp1 negatively regulates dorsal ruffle formation. We also identify WIP as a novel mAbp1-binding partner and show that mutations that abrogate the mAbp1-WIP interaction impair dorsal ruffle formation. Finally we demonstrate that WIP-mediated effects on dorsal ruffle formation require mAbp1 but not cortactin. Taken together, these findings suggest a novel role for mAbp1 in dorsal ruffle formation through its interaction with WIP.

MATERIALS AND METHODS

Reagents and Antibodies

Fibronectin was purified from human plasma by affinity chromatography as described previously (Ruoslahti *et al.*, 1982). DMEM was purchased from Mediatech (Manassas, VA). Ham's F12, Optimem, and rhodamine phalloidin were purchased from Invitrogen (Carlsbad, CA). PDGF-BB was purchased from R&D Systems (Minneapolis, MN) and used at 50 ng/ml. ALLM was purchased from Calbiochem (La Jolla, CA) and used at 100 μg/ml. The following mouse monoclonal antibodies were used: 4F11 anti-cortactin (Upstate Biotechnology, Lake Placid, NY); h-VIN anti-vinculin and anti-Flag (Sigma-Aldrich, St. Louis, MO); anti-GST (Novagen, Madison, WI). Rabbit polyclonal antibodies used were as follows: anti-vinculin (Sigma-Aldrich), anti-N-WASP (Cell Signaling, Beverly, MA), and anti-GFP (Molecular Probes, Eugene, OR). Anti-myc (clone 9E10) was produced from a hybridoma kindly provided by Mary Horn (Ludwig-Maximilians, Germany). Goat polyclonal anti-WIP was purchased from Santa Cruz (Santa Cruz, CA). Antibodies to mouse mAbp1 were generated at the University of Wisconsin Antibody facility by injecting rabbits with full-length GST-mAbp1 bound to glutathione-Sepharose, following standard practice. After immunization and two boosts, IgG was purified using protein A after incubation with glutathione *S*-transferase (GST)-glutathione-Sepharose beads. AlexaFluor 680 goat anti-mouse secondary antibody and AlexaFluor 680 donkey anti-goat IgG secondary antibody were purchased from Molecular Probes. IRDye 800CW goat anti-rabbit IgG secondary antibody was purchased from Rockland Immunochemicals (Gilbertsville, PA). Glutathione-Sepharose was purchased from Amersham Biosciences (Piscataway, NJ). Anti-Flag M2 Agarose was purchased from Sigma.

Cell Culture and Transfection

NIH-3T3 and HEK-293 cells were obtained from the ATCC (Manassas, VA) and cultured according to instructions. NIH-3T3 cells were transfected using Lipofectamine 2000 (Invitrogen) according to manufacturer's instructions. HEK-293 cells were transfected by standard calcium phosphate precipitation. Where indicated, cells were serum-starved for 16–18 h in DMEM containing 0.2% BSA.

Constructs and siRNA

Mouse mAbp1 was kindly provided by David Drubin (University of California-Berkeley). EGFP-actin was purchased from Clontech (Palo Alto, CA). EGFP-cortactin has been described previously (Perrin *et al.*, 2006). Myc-mAbp1 was generated by PCR amplification of mAbp1 with an EcoRI-containing forward primer and an XhoI-containing reverse primer followed by ligation to pcDNA3.1, which contained a myc tag sequence. Mutations were introduced into the calpain cleavage site by site-directed mutagenesis of myc-mAbp1 DNA: D6 primer: 5′CACCACCTCTGGCCTGCAGAAGCAACTC, L289G primer: 5′CAGCCGGGCAAGGGGAGGAGCCCCTTC; the WIP binding site (W415K) of green fluorescent protein (GFP)-mAbp1 primer: 5′GTGATTGACGAAGGCTGGAAGCGAGGCTATGGGCCTG; the mAbp1 binding site (Δ110-170) of GFP-WIP primer: 5′AGGATTGTTCCAGGCTGGAATGCCGCCCCCAAGGCCCGACGTGGGCTCAA or into GFP-mAbp1 to create silent mutations using the QuickChange mutagenesis kit (Stratagene, La Jolla, CA) according to the manufacturer's instructions. GFP-mAbp1 constructs were made by PCR amplification of wild-type or mutant mAbp1 with an EcoRI-containing forward primer and a BamHI-containing reverse primer, followed by ligation to pEGFP-C2 (Clontech). C-terminally Flag-mAbp1 was produced by PCR amplifying mAbp1 with a BamHI-containing forward primer and an XhoI-containing reverse primer that omitted the stop codon and was ligated into pCDNA 3.1-Flag. pCDNA 3.1 Flag was made by annealing a Flag tag oligo containing PstI and XhoI sites into linearized pCDNA 3.1 vector. C-terminally GST-tagged mAbp1 was produced by separately PCR amplifying mAbp1 and GST. mAbp1 was amplified with a BamHI-containing forward primer and an EcoRI-containing reverse primer that omitted the stop codon. GST was amplified from pGEX4T-1 (Amersham Biosciences) using an EcoRI-containing forward primer and a HindIII-containing reverse primer. Both PCR products were simultaneously ligated into pTrcHisA (Invitrogen) that had been digested with BamHI and HindIII, to generate a His-mAbp1-GST fusion. The GFP-mAbp1-N terminal fragment was amplified from full-length pEGFP-mAbp1 with a KpnI-containing forward primer and a BamHI reverse primer that introduced a stop codon. The GFP-mAbp1-C terminal fragment was amplified from full-length pEGFP-mAbp1 with a KpnI-containing forward primer, which introduced a start codon, and a BamHI reverse primer. Both the N- and C-terminal fragments were subsequently ligated into pEGFP-C1 (Clontech). Flag-hWIP was provided by Scott Weed (University of West Virginia). WIP was amplified from pCDNA 3.1 Flag-WIP with a HindIII-containing forward primer and an EcoRI-containing reverse primer and ligated into the pmCherry-C1 vector to make pmCherry-WIP. Cloning of the pmCherry-C1 vector has been previously described (Lokuta *et al.*, 2007). GFP-WIP was constructed by excision of WIP from pmCherry-WIP with HindIII and EcoRI and ligation into pEGFP-C1. N-WASP was amplified with an EcoRI-containing forward primer and an XhoI-containing reverse primer and ligated into pCDNA 3.1-Flag. The pSUPER.retro (OligoEngine, Seattle, WA) RNAi system was utilized to achieve stable expression of short interfering RNAs. Oligonucleotides targeted to mAbp1 mRNA as well as a nonsilencing control were synthesized by Integrated DNA Technologies (Coralville, IA), annealed, and cloned into the pSUPER.retro.puro vector according to manufacturer's instructions. Retroviral transfection was performed as described previously (Franco *et al.*, 2004). Wild type NIH-3T3 cells were infected twice at 32°C for 6 h and allowed to recover in growth medium for 24 h before selection with 1 μg/ml puromycin for 4–5 d. Target sequences for nonsilencing were as follows: for NIH-3T3 cells: control: 5′TTCTCCGAACGTGTCACGT3′; for mAbp1 siRNA: 5′AGAAGAACCTACATATGAA; and for cortactin siRNA: 5′GGAACACATCAACATTCAC. Target sequences for calpain 2 in NIH-3T3 cells have been previously published (Franco *et al.*, 2004). ON-TARGETplus SMARTpool siRNA (Dharmacon, Boulder, CO) was used to knock down WIP in NIH-3T3 cells. Target sequences for mWIP mRNA were 5′CAACATTTGCACTCGCTAA, 5′TGAAATATCACTTCGACTT, 5′CAAACTGGCCAGAAACGAA, and 5′AGGAAAGGCTAGTAGGGCA. ON-TARGET plus Nontargeting siRNA 1 (Dharmacon) was used as a nonsilencing control.

Immunoblot Analysis and Immunoprecipitation

Cells were scraped into lysis buffer (50 mM Tris, pH 7.6, 500 mM NaCl, 0.1% SDS, 0.5% deoxycholate, 1% Triton X-100, 0.5 mM $MgCl_2$, 0.2 mM phenylmethylsulfonyl fluoride [PMSF], 1 μg/ml pepstatin, 2 μg/ml aprotinin, and 1 μg/ml leupeptin) on ice and clarified by centrifugation. Immunoblotting of cell lysates was performed as previously described (Cortesio *et al.*, 2008), and blots were imaged with an Odyssey Infrared Imaging System (Li-Cor Biosciences, Lincoln, NE). For immunoprecipitation (IP) experiments, HEK-293 cells were transfected and lysed 24–48 h later in IP buffer (20 mM HEPES, pH 7.5, 50 mM KCl, 1 mM EDTA, 1% NP40, 0.2 mM PMSF, 1 μg/ml pepstatin, 2 μg/ml aprotinin, and 1 μg/ml leupeptin). Lysates were incubated with 3 μg anti-GFP or 3 μg of rabbit IgG. Immune complexes were captured on GammaBind G Sepharose beads (Amersham Biosciences), washed in lysis buffer, and analyzed by immunoblotting with anti-Flag or anti-GFP antibody. For IP experiments in NIH-3T3 cells, cells were transfected and serum-starved for 18 h. At 24 h, cells were treated with 50 ng/ml PDGF for 8 min, lysed in IP buffer, and immunoprecipitated as above with 3 μg anti-mAbp1 or 20 μl anti-Flag beads. Western blots were analyzed with anti-mAbp1, anti-WIP, anti-Flag, and anti-N-WASP antibodies.

Protein Overlay Assay

FLAG-WIP was generated as described in the TnT T7-coupled reticulocyte lysate system (Promega, Madison, WI). Exogenously expressed GFP, GFP-mAbp1, GFP-W415K-mAbp1, GFP-WIP, or GFP-WIP Δ110-170 were isolated by IP from HEK 293 cells lysed with NP-40 lysis buffer (50 mM HEPES, 75 mM NaCl, 1% NP-40, and 10% glycerol) using 1 μl anti-GFP antibody. Proteins were resolved by SDS-PAGE and transferred to nitrocellulose. Membranes were denatured/renatured by serial washing 15 min each at 4° with 6, 3, 1.5, 0.75, and 0.375 M and 0.188 and 0 M guanidine HCl in a HEPES buffer (25 mM HEPES, 25 mM NaCl, 5 mM $MgCl_2$, and 0.5 mM DTT). The membrane was then blocked with 3% nonfat dry milk in KCl buffer (142.5 mM KCl, 5 mM $MgCl_2$, 10 mM HEPES, and 0.2% NP-40) 1 h at room temperature and then incubated with the FLAG-WIP probe or 1 μg purified His-mAbp1-GST diluted in KCl buffer for 3 h at room temperature. The membrane was then

washed extensively in KCl buffer and blotted with anti-FLAG antibody or anti-GST antibody.

Protein Purification

Mouse mAbp1-GST was purified from *Escherichia coli* (BL21) using glutathione-Sepharose (Amersham Biosciences). Briefly, overnight cultures were diluted 1:10 to fresh LB containing 100 μg/ml ampicillin and 30 μg/ml chloramphenicol and grown at 37°C for 1 h. Expression was induced with 0.4 mM IPTG for 4 h at 37°C. Cells were lysed in TS (10 mM Tris-HCl, pH 7.5, 100 mM NaCl, and 0.2 mM PMSF) by sonication, 1% Triton X-100 was added, the lysate was clarified by centrifugation, and the supernatant was incubated with glutathione-Sepharose beads for 30 min and washed in TS. For antibody production, beads were washed extensively in PBS. His-mAbp1-GST was expressed as above and purified from *E. coli* (BL21) using Ni-NTA metal chelating Sepharose as described previously (Cortesio and Jiang, 2006).

Immunofluorescence

Glass coverslips were acid-washed and coated with 10 μg/ml fibronectin (FN). For dorsal ruffle formation, NIH-3T3 cells were plated on coverslips in DMEM culture medium and were allowed to adhere for 3 h. Cells were serum-starved in DMEM containing 0.2% BSA for 16–18 h. Cells were stimulated with 50 ng/ml PDGF for 10 min. Cells were fixed in 3.7% formaldehyde for 10 min, quenched with 0.15 M glycine for 10 min, permeabilized with 0.2% Triton X-100 for 10 min, and blocked in 5% goat serum. The cells were incubated with primary antibodies or rhodamine phalloidin for 30 min and then with fluorophore-conjugated secondary antibodies for 30 min. Coverslips were imaged using a 60×/1.4 oil objective on an Olympus 1X-70 inverted microscope (Olympus America, Melville, NY). Images were acquired with a Coolsnap fx cooled CCD camera (Photometrics, Huntington Beach, CA) and captured into MetaVue imaging software v6.2 (Universal Imaging, Downingtown, PA). Confocal images were collected using a laser-scanning confocal microscope (Fluoview FV-1000; Olympus) using a 60× Plan Apo/1.45 oil immersion objective with a 2.5 zoom factor and were captured into Fluoview software (FV10-ASW version 01.07; Olympus). Images were processed using MetaMorph software (Universal Imaging). Error bars in all figures represent the SEM of at least three different experiments. Between 50 and 100 cells in each experiment were scored as positive or negative for containing dorsal ruffles.

Time-Lapse Fluorescent Microscopy

Fluorescence imaging of live cells expressing GFP-actin and GFP-cortactin was performed using a 60×/1.40 oil objective on an Olympus 1X-70 inverted microscope. Live imaging of cells expressing GFP-mAbp1 and mCherry-WIP was performed using a 60× objective on a Nikon Eclipse TE300 inverted microscope (Melville, NY). Cells were housed in a closed system to maintain temperature at 37°C. Glass-bottom dishes (35 mm) were coated with 10 μg/ml FN for 1 h at 37°C. For microscopy experiments, cells were plated in DMEM culture media and allowed to adhere for 3 h. Cells were serum-starved in DMEM containing 0.2% BSA for 18 h. Cells were imaged in Ham's F12 medium containing 0.2% BSA, nonessential amino acids, and 20 mM HEPES, pH 7.2, and PDGF (30 ng/ml) was added during image acquisition. Fluorescent images were collected using a Coolsnap fx cooled CCD camera (Photometrics) and captured into MetaVue v6.2 every 30 s for 25 min.

Cleavage Site Mapping

mAbp1-GST on glutathione beads was washed and resuspended in proteolysis buffer (50 mM Tris-HCl, pH 7.5, 134 mM KCl, 1 mM $MgCl_2$, and 1 mM $CaCl_2$). Purified calpain 2 (Sigma) was added to the beads (40–200 μg/ml), and the reaction was incubated at 37°C for 30 min. To analyze the digest, bead volumes were boiled in SDS-PAGE sample buffer, separated on SDS-PAGE gels, and stained with Coomassie blue or immunoblotted. For N-terminal sequencing, beads were washed extensively with TS after digestion with calpain before electrophoresis. Protein was transferred to PVDF membrane (Bio-Rad, Richmond, CA) and stained with Coomassie blue, and an individual band was subjected to sequencing (performed at the Baylor College of Medicine Protein Services Core).

Statistical Analysis

For statistical comparison, the two-tailed, paired, Student's *t* test or one-way ANOVA, with a Tukey post test was used, with $p < 0.05$ considered significant.

RESULTS

mAbp1 Localizes to PDGF-induced Dorsal Ruffles

Growth factor stimulation induces the formation of dynamic and transient circular ruffles on the dorsal surface of NIH-3T3 cells (Mellstrom *et al.*, 1988). To determine if mAbp1 localizes to PDGF-induced circular dorsal ruffles, we generated a polyclonal antibody to mouse Abp1 to detect endogenous mAbp1. In serum-starved NIH-3T3 cells mAbp1 localized both to the peri-nuclear region and the cell periphery. Treatment of the serum-starved cells with PDGF induced dynamic actin remodeling into circular ring shaped structures on the dorsal surface of the cell. We found that endogenous mAbp1 colocalized with actin at PDGF-induced dorsal ruffles (Figure 1A). In accordance with previous reports (Krueger *et al.*, 2003), we also found that cortactin localized with actin at PDGF-induced dorsal ruffles (Figure 1B). Together, these findings identify mAbp1 as a novel component of PDGF-induced dorsal ruffles.

mAbp1 and Cortactin Are Necessary for Dorsal Ruffle Formation

To determine if mAbp1 is necessary for dorsal ruffle formation, we generated a mAbp1-deficient NIH-3T3 cell line by stably expressing mAbp1 siRNA. The knockdown efficiency was ~70% compared with control cells, and cortactin levels were not affected by the mAbp1 siRNA (Figure 2A). Serum-starved mAbp1-deficient cells showed impaired dorsal ruffle formation by more than twofold in the presence of PDGF (Figure 2A). To further characterize the role of mAbp1 during dorsal ruffle formation, we performed time-lapse microscopy to visualize the dynamics of GFP-actin and GFP-cortactin in control and mAbp1-deficient cells in response to PDGF stimulation (Supplemental Videos 1–4). Both GFP-actin and GFP-cortactin localized to dynamic, circular structures on the dorsal cell surface upon PDGF stimulation in

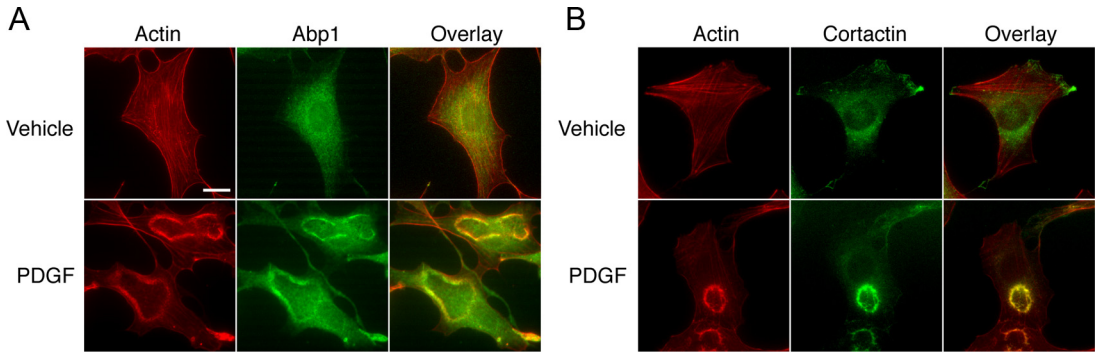

Figure 1. mAbp1 localizes to PDGF-induced dorsal ruffles in fibroblast cells. NIH-3T3 cells were cultured on FN-coated coverslips, serum-starved, and stimulated with vehicle control or PDGF. Cells were fixed and stained with (A) rhodamine phalloidin and anti-mAbp1 antibody or (B) rhodamine phalloidin and anti-cortactin antibody. Bar, 10 μm.

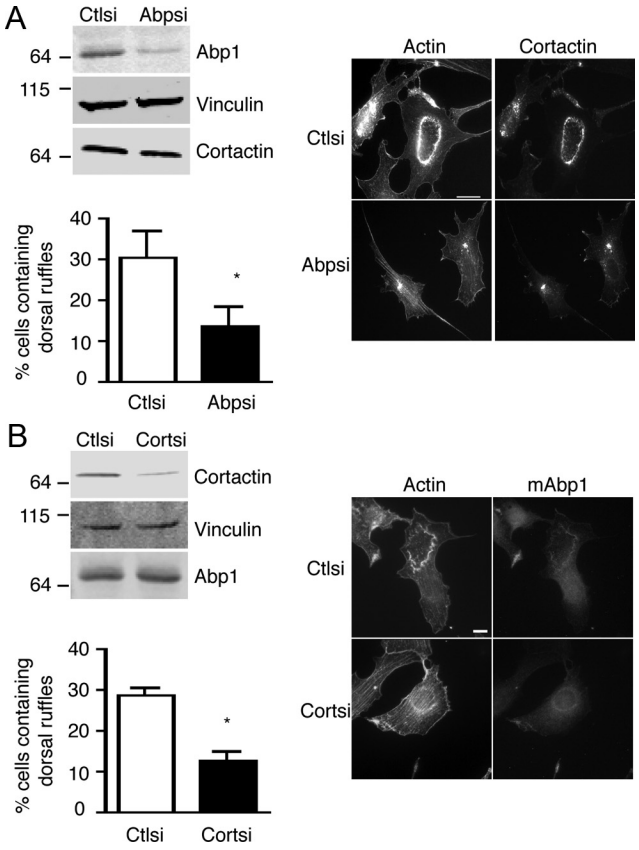

Figure 2. mAbp1 and cortactin are required for dorsal ruffle formation. (A) Representative Western blot of mAbp1 expression in NIH-3T3 cells stably expressing control or mAbp1 siRNA. Cell lysates were analyzed using an anti-mAbp1 antibody (top), anti-vinculin antibody as a loading control (middle), or anti-cortactin antibody (bottom). Western blot shown is representative of at least three independent experiments. Cells expressing control or mAbp1 siRNA were plated on FN-coated coverslips, serum-starved, and stimulated with PDGF. Cells were fixed and stained with rhodamine phalloidin and anti-cortactin antibody. Bar, 10 μm. Dorsal ruffles were quantified by counting the number of cells containing at least one dorsal ruffle after stimulation with PDGF. Greater than 100 cells were counted per condition, and each condition represents the average value from three independent experiments; error bars, SEM; *$p < 0.01$ (Student's t test), compared with Ctlsi. (B) Representative Western blot of cortactin expression in NIH-3T3 cells stably expressing control or cortactin siRNA. Cell lysates were analyzed using an anti-cortactin antibody (top), anti-vinculin antibody as a loading control (middle), or anti-mAbp1 antibody (bottom). Western blot shown is representative of at least three independent experiments. Cells expressing control or cortactin siRNA were plated on FN-coated coverslips, serum-starved, and stimulated with PDGF. Cells were fixed and stained with rhodamine phalloidin and anti-mAbp1 antibody. Dorsal ruffles were quantified by counting the number of cells containing at least one dorsal ruffle after stimulation with PDGF. Greater than 100 cells were counted per condition and each condition represents the average value from three independent experiments; error bars, SEM; *$p < 0.01$ (Student's t test), compared with Ctlsi.

control cells. These structures varied in size and number, with an average duration of ~6 min. In contrast, mAbp1-deficient cells showed impaired dorsal ruffle formation, and the dorsal ruffles that formed were smaller with a reduced average duration of ~4.5 min (Supplemental Videos 1–4 and data not shown).

Previous work has demonstrated the importance of a cortactin-dynamin 2 interaction in dorsal ruffle formation (Krueger *et al.*, 2003). To further examine the importance of cortactin in dorsal ruffle formation, we generated a cortactin-deficient NIH-3T3 cell line by stably expressing cortactin siRNA. The knockdown efficiency was ~75% compared with control cells, and mAbp1 levels were not affected by the cortactin siRNA (Figure 2B). Serum-starved, cortactin-deficient cells showed impaired dorsal ruffle formation by more than twofold in the presence of PDGF (Figure 2B), comparable to the effects observed with mAbp-1 depletion. Together, these findings indicate that both mAbp1 and cortactin are necessary for the formation of dorsal ruffles in growth factor–treated cells.

mAbp1 and Cortactin Have Nonredundant Functions in Dorsal Ruffle Formation

To determine if mAbp1 and cortactin have redundant functions in dorsal ruffle formation, GFP-mAbp1, GFP-cortactin, or GFP alone were transiently expressed in mAbp1- or cortactin-deficient NIH-3T3 cells (Figure 3). mAbp1 and cortactin knockdown cells expressing GFP alone exhibited a greater than twofold reduction in dorsal ruffle formation compared with control cells upon growth factor stimulation (Figure 3). Expression of GFP-mAbp1 in mAbp-deficient cells or GFP-cortactin in cortactin-deficient cells rescued dorsal ruffle formation to levels approximately equal to control cells (Figure 3). Expression of GFP-mAbp1 was unable to rescue dorsal ruffle formation in cortactin-deficient cells. Similarly, GFP-cortactin was unable to rescue dorsal ruffle formation in mAbp1-deficient cells, suggesting that cortactin and mAbp1 have nonredundant functions in dorsal ruffle formation.

Calpain 2 Proteolysis of mAbp1 Negatively Regulates Dorsal Ruffle Formation

Previous studies have demonstrated that calpain-mediated proteolysis of cortactin regulates the dynamics of actin-based structures including lamellipodia formation (Perrin *et al.*, 2006) and invadopodia dynamics (Cortesio *et al.*, 2008). Because cortactin and mAbp1 are structurally similar, we hypothesized that mAbp1 function may be similarly regulated by calpain-mediated proteolysis. mAbp1 proteolysis was observed in control NIH-3T3 cells with the generation of a fragment of ~30 kDa. Calpain 2–deficient NIH-3T3 cells did not show significant mAbp1 proteolysis, suggesting that calpain 2 also cleaves mAbp1 (Figure 4A). To confirm calpain 2 proteolysis of mAbp1, we incubated purified mAbp1-GST with increasing concentrations of calpain 2. Consistent with the results in cultured fibroblasts, calpain 2 treatment in vitro generated a prominent cleavage fragment of a similar molecular weight (Figure 4B). Because calpain cleavage sites are not defined by a consensus primary amino acid sequence (Tompa *et al.*, 2004), we mapped the calpain cleavage site in mAbp1, using N-terminal sequencing. Sequencing revealed two fragments that were generated by calpain 2 proteolysis at two separate sites within a nine-amino acid region that is located between the charged-helical F-actin–binding domain and the proline-rich domain (Figure 4C and Supplemental Figure 1A).

To verify the cleavage sites and to generate a calpain-resistant mutant of mAbp1, we made several deletion and point mutations in the mapped region (Supplemental Figure 1B). Of the mutants we generated, mAbp1-D6-L289G contained the most conservative mutations that resulted in decreased susceptibility to calpain 2–mediated proteolysis and was used for subsequent experimental analysis (Supplemental Figure 1C). To determine if calpain-mediated proteolysis of mAbp1 is important in dorsal ruffle formation, cells stably expressing con-

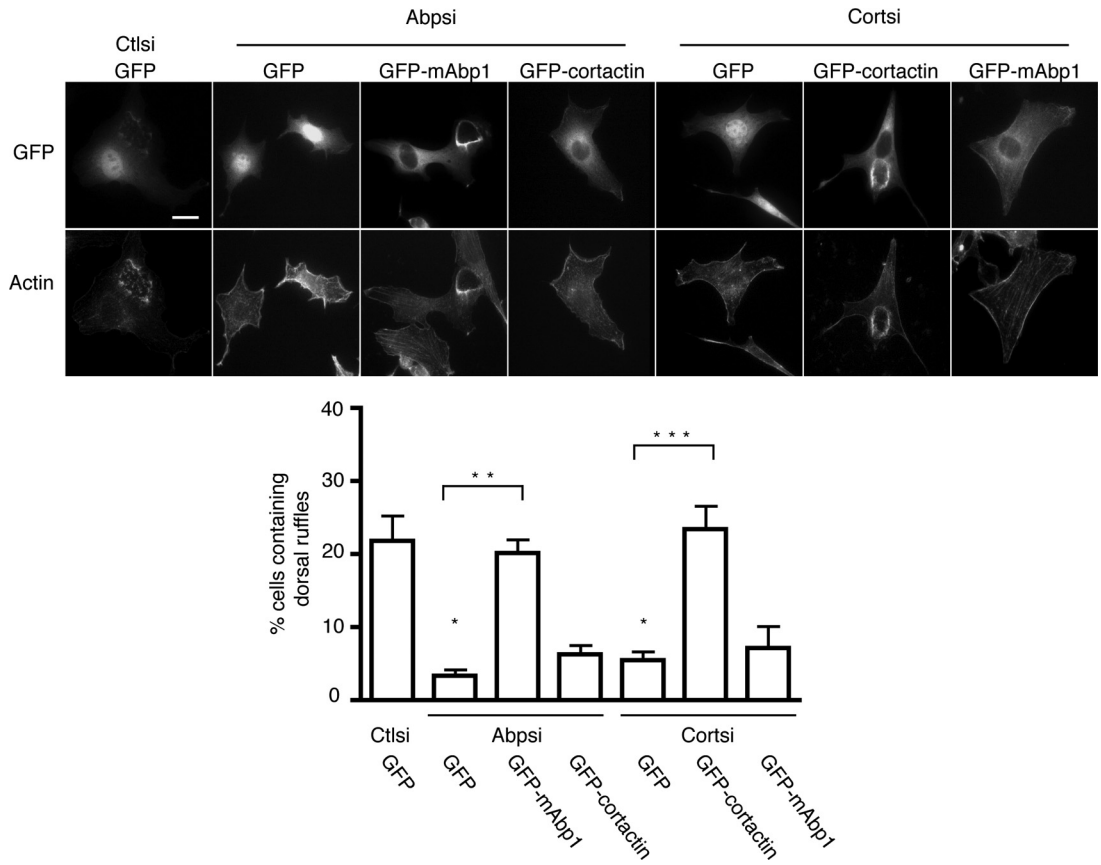

Figure 3. mAbp1 and cortactin have nonredundant functions in dorsal ruffle formation. NIH-3T3 cells stably expressing control, mAbp1, or cortactin siRNA were transiently transfected with GFP, GFP-mAbp1, or GFP-cortactin. Cells were plated on FN-coated coverslips, serum-starved, and stimulated with PDGF. Cells were fixed and stained with rhodamine phalloidin. Bar, 10 μm. Dorsal ruffles were quantified by counting the number of GFP-positive cells containing at least one dorsal ruffle after stimulation with PDGF. Greater than 50 cells were counted per condition, and each condition represents the average value from three independent experiments; error bars, SEM; *$p < 0.01$, compared with Ctlsi GFP, **$p < 0.001$ compared with Abpsi GFP, and ***$p < 0.001$ compared with Cortsi GFP by one-way ANOVA.

trol or mAbp1 siRNA were transiently transfected with GFP, wild-type GFP-mAbp1, or GFP-mAbp1-D6-L289G. In accordance with our previous data, mAbp1-deficient cells expressing GFP alone showed impaired dorsal ruffle formation compared with control cells. Dorsal ruffle formation in mAbp1-deficient cells was rescued by expression of wild-type GFP-mAbp1 and the calpain-resistant mAbp1 (Supplemental Figure 1D), suggesting that calpain proteolysis is not necessary for the formation of dorsal ruffles.

To further examine how calpain-mediated proteolysis of mAbp1 regulates dorsal ruffle formation, we constructed GFP-tagged N- and C-terminal mAbp1 fragments corresponding to the calpain 2 cleavage products (Figure 4C). Expression of either the GFP-tagged N- or C-terminal fragments in mAbp1-deficient cells was not sufficient to rescue dorsal ruffle formation, demonstrating that the mAbp1 actin-binding domains or the proline rich/SH3 domains alone are not able to rescue dorsal ruffle formation (data not shown). To determine if the calpain-generated fragments have an inhibitory effect on dorsal ruffle formation, parental NIH-3T3 cells were transiently transfected with GFP, wild-type GFP-mAbp1, GFP-N-terminal or C-terminal mAbp1 fragments and treated with PDGF to induce dorsal ruffle formation (Figure 4D). Expression of wild-type or the N-terminal fragment of mAbp1 had minimal effects on dorsal ruffle formation compared with control cells (Figure 4D). In contrast, expression of the C-terminal mAbp1 fragment decreased dorsal ruffle formation by approximately threefold (Figure 4D). These findings suggest that the C-terminal calpain proteolytic fragment plays an inhibitory role in dorsal ruffle formation. Interestingly, calpain-mediated proteolysis of mAbp1 was enhanced in PDGF-treated NIH-3T3 cells at time points greater than 30 min when dorsal ruffles no longer form in response to growth factor (Supplemental Figure 2), suggesting that PDGF-induced proteolysis of mAbp1 may contribute to the cessation of dorsal ruffle formation after PDGF stimulation. Together, these data implicate calpain-mediated proteolysis of mAbp1 as a mechanism that may negatively regulate dorsal ruffle formation.

mAbp1 and WIP Localize to PDGF-induced Dorsal Ruffles

Previous studies have demonstrated that the WASP-binding protein, WIP, is necessary for dorsal ruffle formation (Anton *et al.*, 2003). We also find that NIH-3T3 cells transiently expressing WIP siRNA are impaired in their ability to form dorsal ruffles (Supplemental Figure 3). To determine if mAbp1 and WIP colocalize in PDGF-induced dorsal ruffles, GFP-mAbp1 and mCherry-WIP were coexpressed in NIH-3T3 cells, and dual, time-lapse microscopy was used to visualize their dynamics (Figure 5A). Both GFP-mAbp1 and mCherry-WIP localized to circular structures on the dorsal surface upon PDGF stimulation and exhibited similar dynamics with rapid translocation to dorsal ruffles induced by

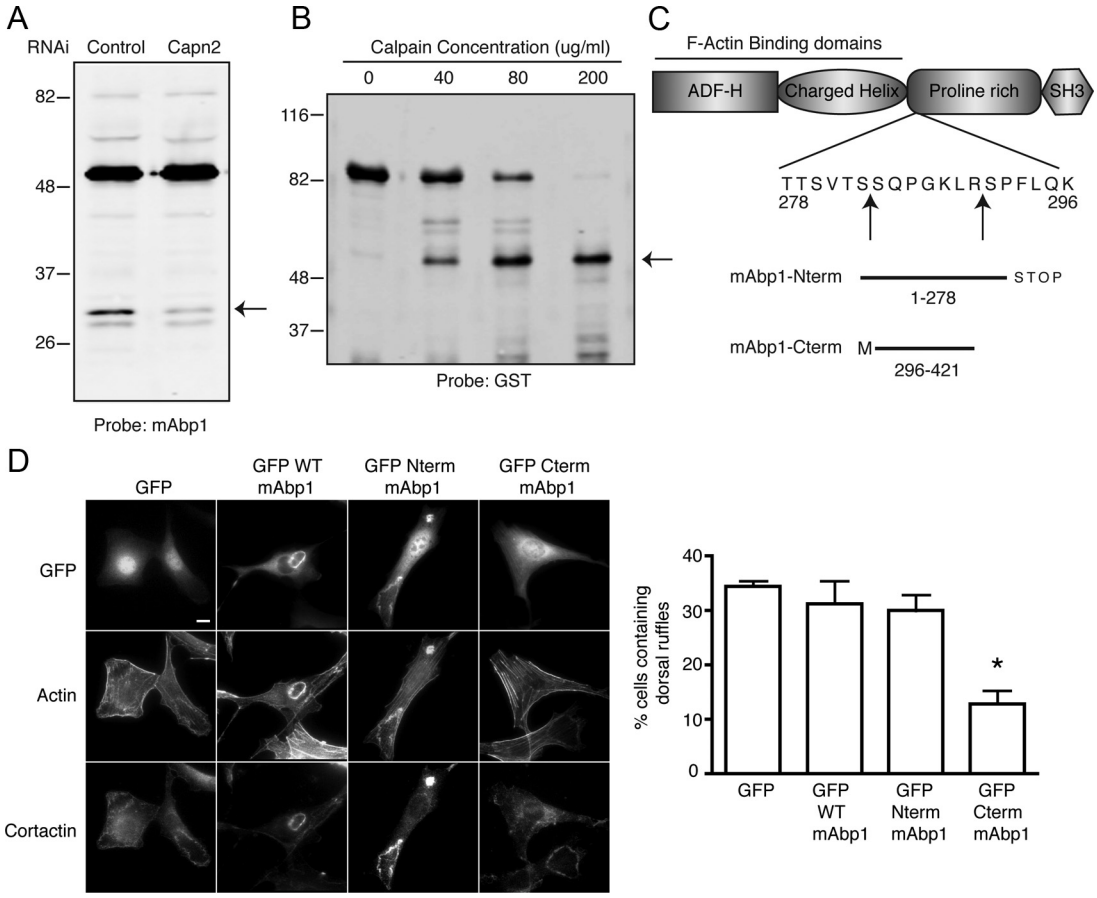

Figure 4. The calpain 2–mediated proteolytic fragment of mAbp1 negatively regulates dorsal ruffle formation. (A) Immunoblot analysis of endogenous mAbp1. Lysates from NIH-3T3 fibroblasts expressing control or calpain 2–specific siRNA were blotted and probed using an antibody against mouse mAbp1. The arrow indicates the calpain-dependent cleavage fragment. Western blot shown is representative of at least three independent experiments. (B) In vitro cleavage of mAbp1-GST. mAbp1-GST bound to glutathione-Sepharose beads was incubated with increasing concentrations of purified calpain 2. The reaction mixture was immunoblotted with anti-GST antibody. The arrow indicates the band that was analyzed by N-terminal sequencing. Western blot shown is representative of at least three independent experiments. (C) Schematic of mAbp1. Arrows indicate the sites of calpain proteolysis identified by N-terminal sequencing. N- and C-terminal mAbp1 constructs were made, corresponding to the calpain 2 cleavage fragments. (D) Parental NIH-3T3 cells were transiently transfected with GFP, GFP-mAbp1, GFP-N-terminal-mAbp1, or GFP-C-terminal-mAbp1. Cells were plated on FN-coated coverslips, serum-starved, and stimulated with PDGF. Cells were fixed and stained with rhodamine phalloidin and anti-cortactin antibody. Bar, 10 μm. Dorsal ruffles were quantified by counting the number of GFP-positive cells containing at least one dorsal ruffle after stimulation with PDGF. Greater than 50 cells were counted per condition, and each condition represents the average value from three independent experiments; error bars, SEM; *$p < 0.01$, compared with GFP control by one-way ANOVA.

PDGF (Figure 5A and Supplemental Video 5). To further confirm that WIP and mAbp1 colocalize at dorsal ruffles, GFP-WIP was transiently expressed in NIH-3T3 cells and circular dorsal ruffles were induced with PDGF. Both GFP-WIP and endogenous mAbp1 localized with the dorsal ruffle markers actin and cortactin in circular structures found on the dorsal surface of the cell by confocal microscopy (Figure 5B and data not shown).

Next we determined if WIP expression could rescue the impaired dorsal ruffle formation induced by expression of the C-terminal fragment of mAbp1. mCherry-WIP was coexpressed with the GFP-C-terminal fragment of mAbp1 in NIH-3T3 cells and stimulated with PDGF to induce dorsal ruffle formation (Figure 5C). Expression of the GFP-C-terminal fragment of mAbp1 impaired dorsal ruffle formation in comparison to control cells by threefold, and coexpression of mCherry-WIP rescued dorsal ruffle formation to control levels (Figure 5C).

mAbp1 Binds to WIP through Its SH3 Domain

WIP binds to the SH3 domain of several proteins that mediate dorsal ruffle formation including N-WASP and cortactin (Kinley *et al.*, 2003; Anton *et al.*, 2007). Because the mAbp1 SH3 domain is similar to the cortactin SH3 domain, we determined whether mAbp1 also binds WIP. A mutation in the cortactin SH3 domain blocks binding of cortactin to WIP (Kinley *et al.*, 2003). An analogous mutation, W415K, was introduced into the SH3 domain of mAbp1 (Figure 6A). GFP-mAbp1 or GFP-mAbp1 W415K were coexpressed in HEK-293 cells with Flag-WIP, and mAbp1 was immunoprecipitated with GFP antibody. We found that Flag-WIP specifically coimmunoprecipitated with GFP-mAbp1 but not GFP-mAbp1-W415K or GFP alone (Figure 6B), suggesting that mAbp1 interacts with WIP through its SH3 domain. To determine if the interaction between WIP and mAbp1 was direct, a protein overlay assay was performed. A Flag-WIP probe bound to immobilized wild-type GFP-Abp1 but not

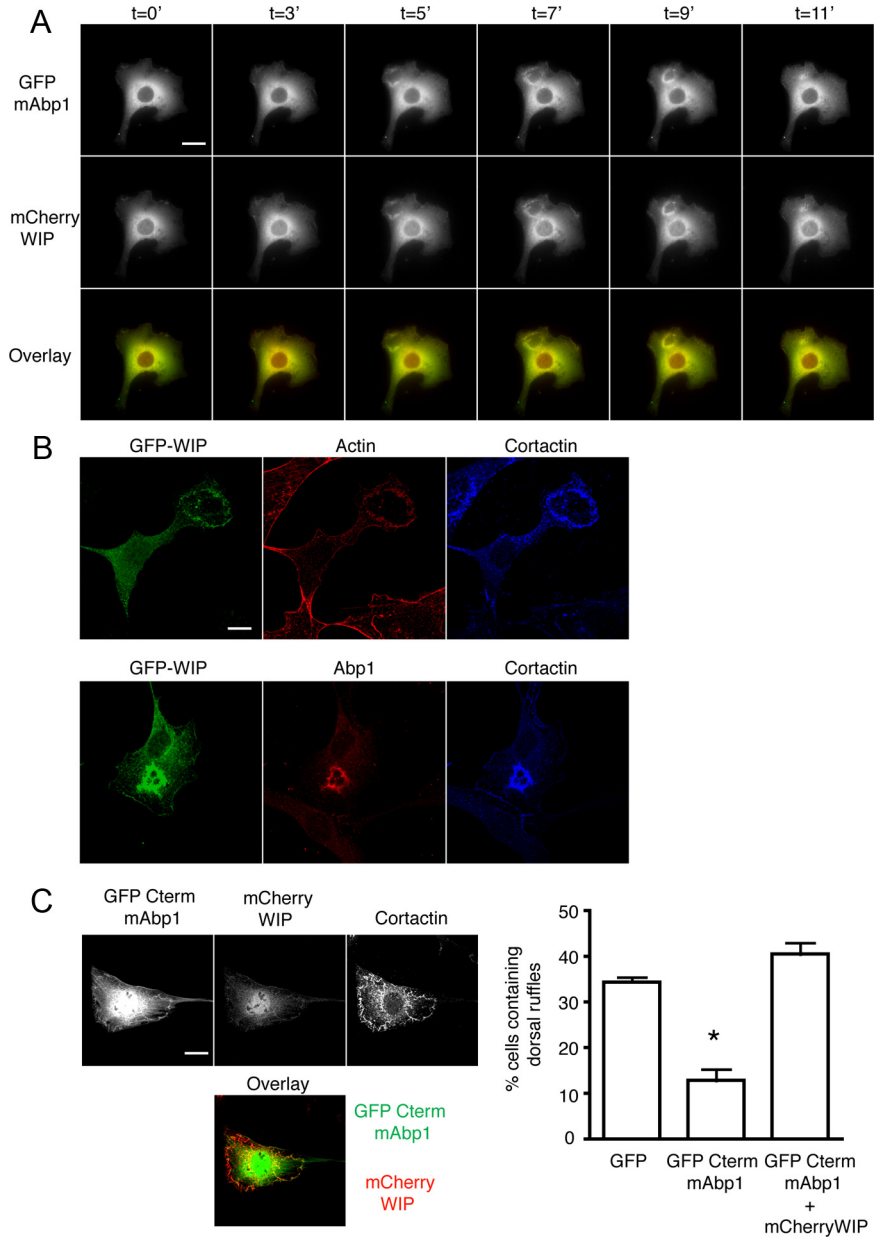

Figure 5. mAbp localizes with WIP at dorsal ruffles. (A) GFP-mAbp1 and mCherry-WIP were transiently transfected into NIH-3T3 cells. Cells were plated on FN-coated, glass-bottomed dishes and serum-starved. Cells were stimulated with PDGF and subsequently analyzed by dual, time-lapse fluorescence microscopy. Montages are representative of at least three independent experiments. Bar, 10 μm. See accompanying Video 5. (B) GFP-WIP was transiently transfected into NIH-3T3 cells. Cells were plated on FN-coated coverslips, serum-starved, and stimulated with PDGF. Cells were fixed and stained with rhodamine phalloidin and anti-cortactin antibody (top panel) or anti-mAbp1 and anti-cortactin antibodies (bottom panel). Bar, 10 μm. (C) NIH-3T3 cells were transiently transfected with GFP, GFP-C-terminal mAbp1, or GFP-C-terminal mAbp1 and mCherry WIP. Cells were plated on FN-coated coverslips, serum-starved, and stimulated with PDGF. Cells were fixed and stained with anti-cortactin antibody. A representative image of a GFP-C-terminal mAbp1 coexpressing mCherry-WIP is shown (left). Bar, 10 μm. Dorsal ruffles were quantified by counting the number of transfected cells containing at least one dorsal ruffle after stimulation with PDGF. Greater than 50 cells were counted per condition, and each condition represents the average value from three independent experiments; error bars, SEM; *$p < 0.01$ compared with GFP control by one-way ANOVA.

GFP-W415K mAbp1 or GFP alone (Figure 6C), suggesting that WIP and mAbp1 interact directly through the mAbp1 SH3 domain. To determine if the interaction between WIP and mAbp1 is regulated by PDGF, Flag-WIP was expressed in NIH-3T3 cells and immunoprecipitated with anti-Flag agarose (Figure 6D). We found that endogenous mAbp1 specifically coimmunoprecipitated with Flag-WIP and that this interaction was enhanced approximately twofold with PDGF treatment (Figure 6D). N-WASP was also found to coimmunoprecipitate with Flag-WIP, but in contrast to the mAbp1-WIP interaction was not enhanced with PDGF treatment (Figure 6D). To confirm the mAbp1-WIP interaction, endogenous mAbp1 was immunoprecipitated from NIH-3T3 cells using our anti-mAbp1 antibody (Figure 6E). We found that endogenous WIP coimmunoprecipitated with mAbp1 and that this interaction was enhanced upon PDGF treatment (Figure 6E). Together, these findings indicate that mAbp1 and WIP interact directly and that the interaction is regulated by PDGF.

mAbp1 Mediates Dorsal Ruffle Formation through Its SH3 Domain

To determine how mAbp1 regulates dorsal ruffle formation, cells stably expressing control or mAbp1 siRNA were transiently transfected with GFP, wild-type GFP-mAbp1, or GFP-mAbp1-W415K and treated with PDGF to induce dorsal ruffle formation (Figure 7A). Dorsal ruffle formation in mAbp1-deficient cells was rescued by expression of wild-type GFP-mAbp1 but not GFP-mAbp1-W415K, suggesting that the mAbp1 SH3 domain is necessary for dorsal ruffle formation (Figure 7A).

To determine if the inhibitory effects of the C-terminal mAbp1 fragment on dorsal ruffles required the ability to bind WIP, the W415K mutation was introduced into the GFP-C-terminal mAbp1 fragment. Parental NIH-3T3 cells were transiently transfected with GFP, GFP-C-terminal mAbp1, or GFP-C-terminal mAbp1-W415K. In accordance with our previous data (Figure 4D), the GFP-C-terminal

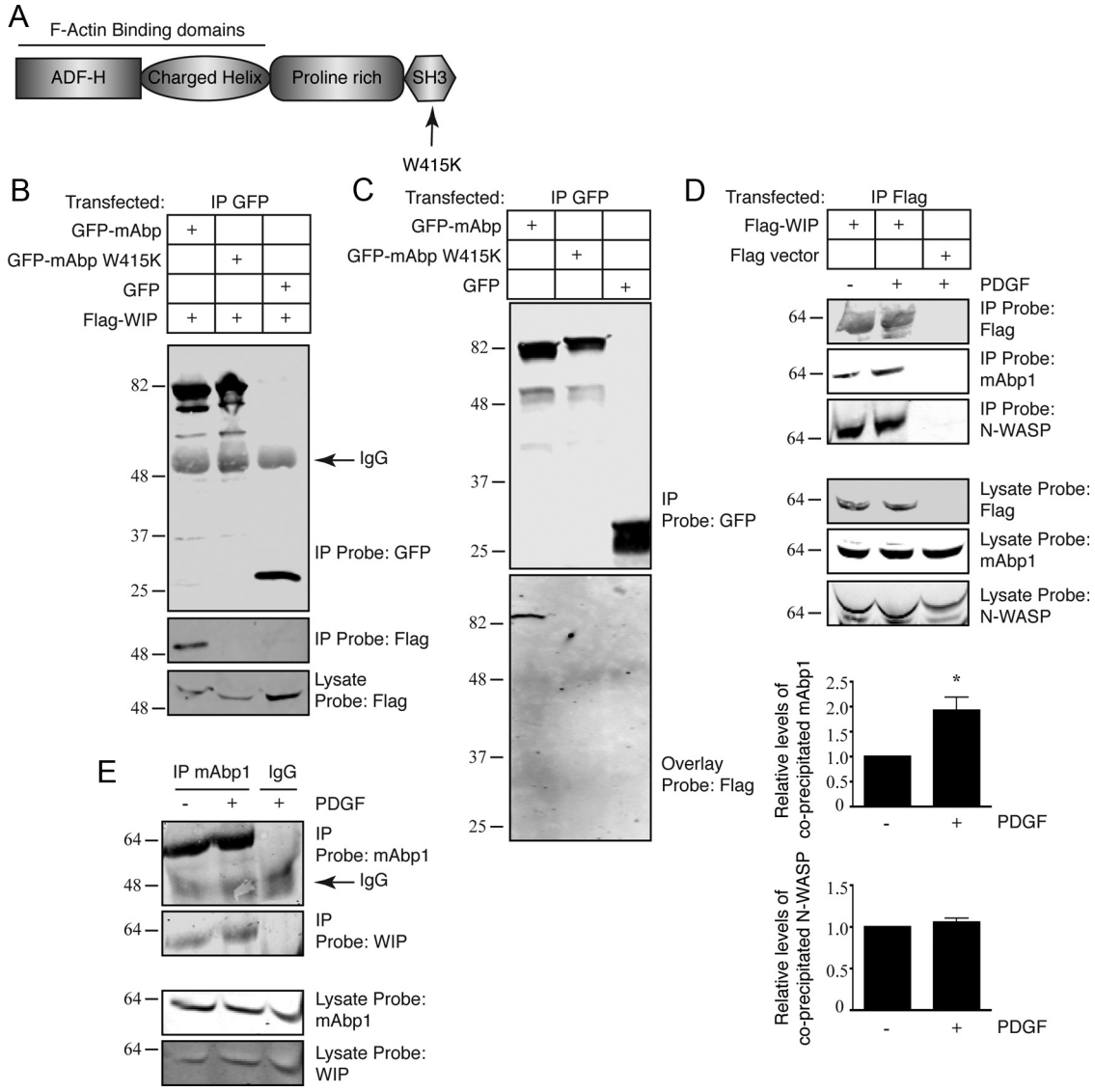

Figure 6. mAbp1 interacts with WIP through its SH3 domain. (A) Schematic of mAbp1. Arrow indicates the mutation, W415K, introduced into the SH3 domain of mAbp1. (B) HEK-293 cells were transfected with GFP, GFP-mAbp1, or GFP-mAbp1 containing a W415K mutation in the SH3 domain, in combination with Flag-WIP. Protein was immunoprecipitated with anti-GFP antibody, separated by SDS-PAGE, and probed with anti-GFP antibody to detect mAbp1 or anti-Flag antibody to detect WIP. Western blot shown is representative of at least three independent experiments. (C) HEK-293 cells were transfected with GFP, GFP-mAbp1, or GFP-mAbp1 containing a W415K mutation in the SH3 domain. Protein was immunoprecipitated with anti-GFP antibody, separated by SDS-PAGE, and probed with anti-GFP antibody (top). The immobilized, immunoprecipitated proteins were incubated with a FLAG-WIP probe and blotted with anti-FLAG antibody (bottom). Western blot and overlay data shown are representative of at least three independent experiments. (D) NIH-3T3 cells were transfected with Flag-WIP or vector control. Transfected cells were serum-starved and treated with vehicle control or PDGF. Protein was immunoprecipitated with anti-Flag agarose, separated by SDS-PAGE, and probed with anti-Flag antibody to detect WIP, anti-mAbp1, and anti-N-WASP antibodies. Levels of mAbp1 or N-WASP that coimmunoprecipitated with Flag-WIP were quantified. Western blot and quantification shown are representative of four independent experiments. (E) NIH-3T3 cells were serum-starved and treated with vehicle control or PDGF. Protein was immunoprecipitated with anti-mAbp1 antibody, separated by SDS-PAGE and probed with anti-mAbp1 and anti-WIP antibodies. Western blot shown is representative of two independent experiments.

mAbp1 fragment inhibited dorsal ruffle formation; however, the GFP-C-terminal mAbp1-W415K did not inhibit dorsal ruffles (Figure 7B). Taken together, these findings support a novel role for mAbp1 in PDGF-induced dorsal ruffle formation through an interaction with WIP at dorsal ruffles.

WIP Effects on Dorsal Ruffle Formation Require mAbp1

To further investigate the importance of a mAbp-WIP interaction in the formation of dorsal ruffles, several WIP deletion constructs were made and tested for their ability to bind mAbp1 by a protein overlay assay (Figure 8, A and B, and data not shown). A 60-amino acid deletion in the N-terminal region of the WIP proline-rich domain, Δ110-170, abrogated the mAbp1-WIP interaction by more than 70% (Figure 8B), yet retained the ability to bind N-WASP (Supplemental Figure 4).

To determine if WIP binding to mAbp1 was important for dorsal ruffle formation, we overexpressed wild-type WIP and the WIP deletion mutant (Δ110-170) in NIH-3T3 cells.

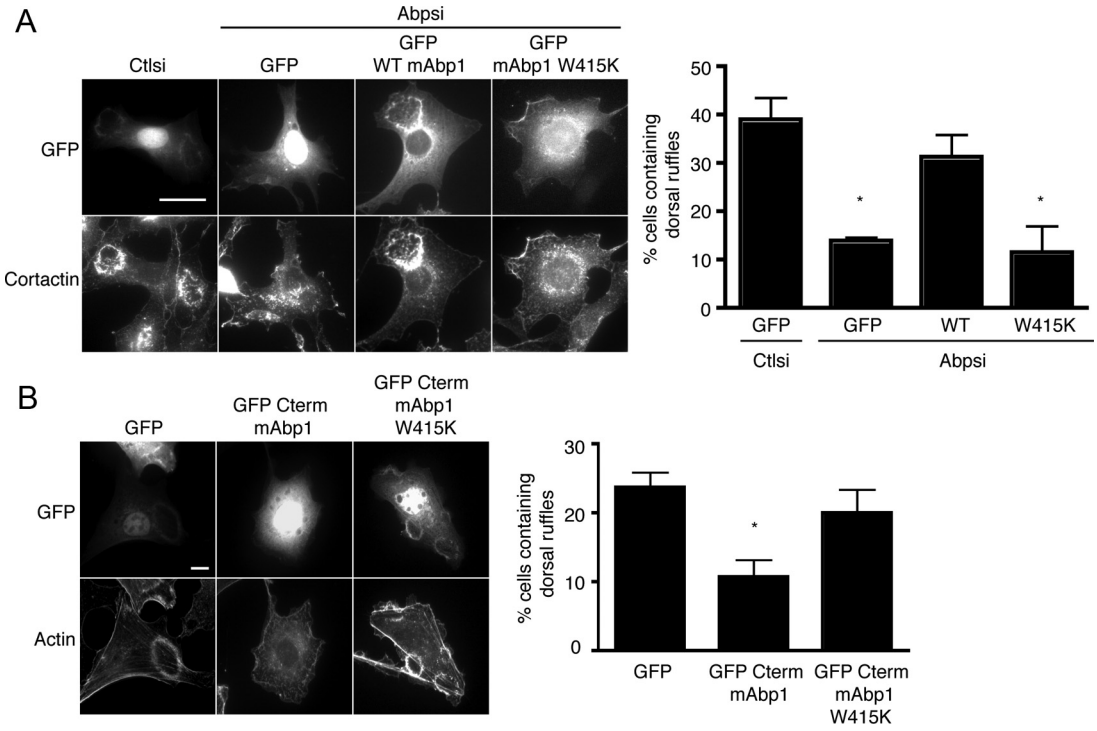

Figure 7. The mAbp1 W415K mutant is unable to rescue dorsal ruffle formation in mAbp1 knockdown cells. (A) NIH-3T3 cells stably expressing control or mAbp1 siRNA were transiently transfected with GFP, WT GFP-mAbp1, or GFP-mAbp1-W415K and plated on FN-coated coverslips, serum-starved, and stimulated with PDGF. Cells were fixed and stained with anti-cortactin antibody. Bar, 10 μm. Dorsal ruffles of GFP-positive cells were quantified by counting the number of cells containing at least one dorsal ruffle after stimulation with PDGF. Greater than 50 cells were counted per condition, and each condition represents the average value from three independent experiments; error bars, SEM; *$p < 0.01$ compared with Ctlsi GFP by one-way ANOVA. (B) Parental NIH-3T3 cells were transiently transfected with GFP, GFP-C-terminal-mAbp1 or GFP-C-terminal-mAbp1-W415K. Cells were plated on FN-coated coverslips, serum-starved, and stimulated with PDGF. Cells were fixed and stained with rhodamine phalloidin. Bar, 10 μm. Dorsal ruffles were quantified by counting the number of GFP-positive cells containing at least one dorsal ruffle after stimulation with PDGF. Greater than 50 cells were counted per condition, and each condition represents the average value from three independent experiments; error bars, SEM; *$p < 0.01$, compared with GFP control by one-way ANOVA.

Previous studies have reported that ectopic expression of wild-type WIP increases dorsal ruffle formation in PDGF-treated NIH-3T3 cells (Anton *et al.*, 2003). In accordance with previous reports, wild-type WIP resulted in increased PDGF-induced dorsal ruffle formation compared with GFP control cells. In contrast, ectopic expression of the Δ110-170 WIP deletion construct that is impaired in mAbp1 binding did not result in increased dorsal ruffle formation (Figure 8C).

To determine if WIP-mediated dorsal ruffle formation requires mAbp1 or cortactin, GFP alone or wild-type GFP-WIP was transiently expressed in control, mAbp1 or cortactin-deficient NIH-3T3 cells (Figure 9). Expression of GFP-WIP enhanced PDGF-induced dorsal ruffle formation in control cells and cortactin-deficient cells but not in mAbp1-deficient cells (Figure 9), suggesting that mAbp1, but not cortactin, is necessary for WIP-mediated dorsal ruffle formation.

DISCUSSION

In this study we identify a novel role for the actin-binding protein mAbp1 in the formation of dorsal ruffles. Dorsal ruffle formation was impaired more than twofold in mAbp1-deficient cells, similar to the phenotype observed in both cortactin and WIP-deficient cells. This is the first study to identify mAbp1 as a calpain substrate and as a novel WIP binding partner. Despite having similar binding partners and modes of regulation, we show that mAbp1 and cortactin have nonredundant functions in dorsal ruffle formation. Interestingly, calpain-mediated proteolysis of mAbp1 is not necessary for the formation of dorsal ruffles but instead may negatively regulate dorsal ruffle formation through the generation of an inhibitory C-terminal mAbp1 fragment. Our findings demonstrate that a critical determinant of mAbp1 function in dorsal ruffle formation is mediated through its SH3 domain, likely through its interaction with WIP. Finally, WIP-mediated effects on dorsal ruffles in NIH-3T3 cells require mAbp1, but not cortactin. Taken together, our findings identify a novel role for mAbp1 in growth factor–induced dorsal ruffle formation through its interaction with WIP.

Growth factor-induced dorsal ruffles have been implicated in diverse cellular processes including the endocytosis of growth factor receptors (Krueger *et al.*, 2003; Orth *et al.*, 2006), dissolution of actin-containing stress fibers (Orth *et al.*, 2006), and macropinocytosis (Warn *et al.*, 1993). The signaling pathways that mediate the dynamics of dorsal ruffles have been the focus of recent investigation. Several signaling pathways have been implicated in the formation of dorsal ruffles including Src family kinases (Veracini *et al.*, 2006), RhoGTPases and PI3-kinase (Suetsugu *et al.*, 2003). Furthermore, the GTPase dynamin has been shown to be critical for growth factor stimulated dorsal ruffles through its interaction with cortactin (Krueger *et al.*, 2003). Here we demonstrate that mAbp1 is necessary for efficient dorsal ruffle formation. It is particularly interesting that despite their

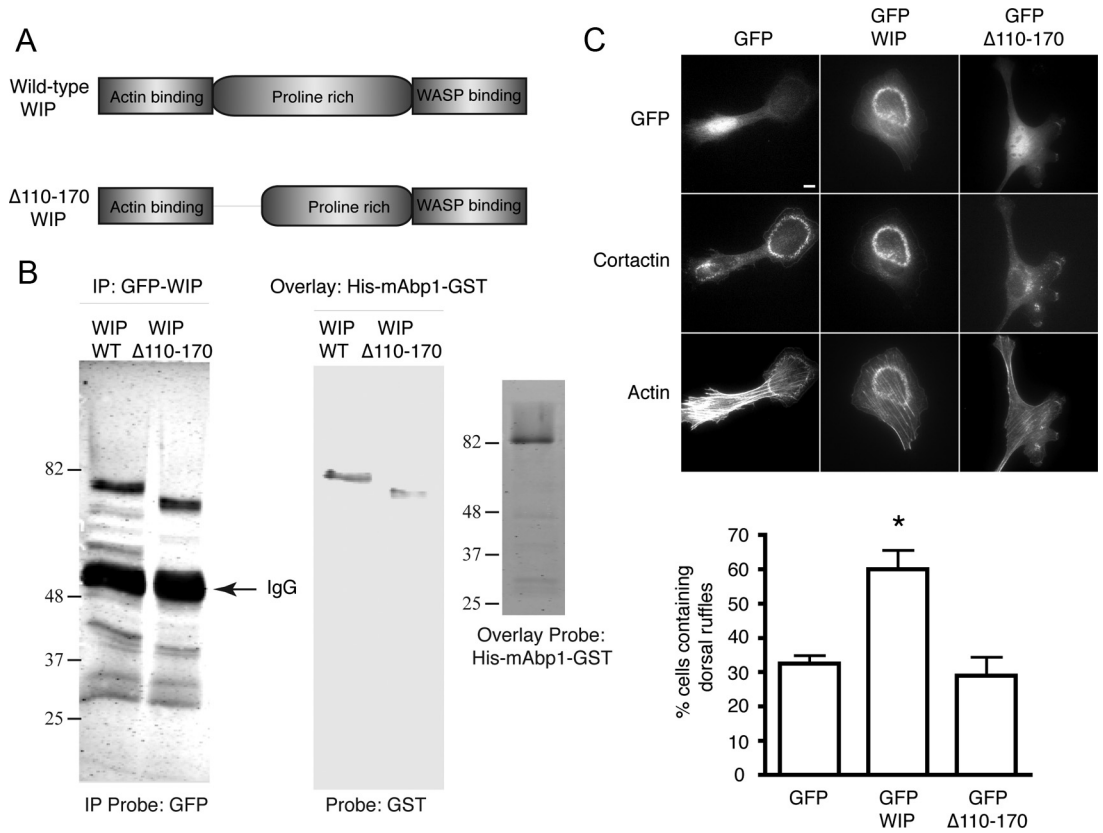

Figure 8. A WIP mutant deficient in mAbp1 binding is unable to induce dorsal ruffle formation. (A) Schematic of wild-type WIP and a mutant WIP, Δ110-170, where the solid line represents a deletion of 60 amino acids in the proline-rich domain. (B). HEK-293 cells were transfected with GFP-WIP or GFP-WIP Δ110-170. Protein was immunoprecipitated with anti-GFP antibody, separated by SDS-PAGE, and probed with anti-GFP antibody (left). The immobilized, immunoprecipitated proteins were incubated with purified His-mAbp1-GST protein and blotted with anti-GST antibody (middle). Western blot and overlay data shown are representative of at least three independent experiments. The purified probe, His-mAbp1-GST (2 μg), was analyzed by Coomassie stain (right). (C) NIH-3T3 cells were transiently transfected with GFP, GFP-WIP, or GFP-WIP Δ110-170 and plated on FN-coated coverslips, serum-starved, and stimulated with PDGF. Cells were fixed and stained with rhodamine phalloidin and anti-cortactin antibody. Bar, 10 μm. Dorsal ruffles of GFP-positive cells were quantified by counting the number of cells containing at least one dorsal ruffle after stimulation with PDGF. Greater than 50 cells were counted per condition, and each condition represents the average value from three independent experiments; error bars, SEM; *$p < 0.01$ compared with GFP control by one-way ANOVA.

structural similarities, mAbp1 and cortactin have nonredundant roles in the regulation of dorsal ruffles.

Recent studies have demonstrated that several proteins that regulate the actin cytoskeleton are calpain substrates. Calpain 2–mediated proteolysis of cortactin regulates both membrane protrusion (Perrin *et al.*, 2006) and invadopodia dynamics (Cortesio *et al.*, 2008). Furthermore the downstream Rac effectors that stimulate Arp 2/3-dependent actin polymerization, WAVE1, WAVE2 and WAVE 3, are also subject to calpain-mediated proteolysis (Oda *et al.*, 2005). Together, these findings suggest that actin regulatory proteins are an important class of calpain substrates. Calpain-mediated proteolysis of mAbp1 separates the F-actin–binding domain and the SH3 domain. Interestingly, expression of the SH3 domain–containing fragment of mAbp1 inhibited dorsal ruffle formation, likely through its association with WIP because WIP overexpression rescued the phenotype (Figure 5C). It is possible that calpain proteolysis of mAbp1 may also be important for regulating other processes mediated by mAbp1, such as vesicle trafficking. This merits further study since calpains have been implicated in synaptic vesicle assembly and budding as well as endosomal recycling and vesicle fusion during exocytosis (Evans and Turner, 2007). Interestingly, cortactin is also cleaved between the F-actin–binding domain and the SH3 domain, suggesting that mAbp1 and cortactin are similarly regulated by calpain proteases. Furthermore, the proline-rich domains of mAbp1 and cortactin are also both phosphorylated by Src-family kinases and in vitro evidence suggests phosphorylation of cortactin results in increased susceptibility to calpain proteolysis (Huang *et al.*, 1997). In the future it will be interesting to determine if Src signaling affects the calpain-mediated proteolysis of mAbp1.

Although yeast Abp1 binds directly to Arp 2/3 to activate its actin nucleation activity, mAbp1 lacks the canonical sequences required for Arp 2/3 binding (Schafer, 2002). However, it has been postulated that mAbp1 may promote Arp 2/3 activity through an alternative mechanism. Our data support the interesting possibility that mAbp1 may regulate Arp 2/3 activity and thereby dorsal ruffle formation through binding WIP. Accordingly, a role for WIP in the organization of the actin cytoskeleton has been previously established. WIP interacts directly with both actin and N-WASP (Martinez-Quiles *et al.*, 2001). Furthermore, WIP-deficient fibroblasts have decreased PDGF-induced dorsal ruffle formation (Anton *et al.*, 2003) and N-WASP–mediated activation of Arp 2/3 is necessary for dorsal ruffle formation (Legg *et al.*, 2007). However, WIP-mediated dorsal ruffle formation

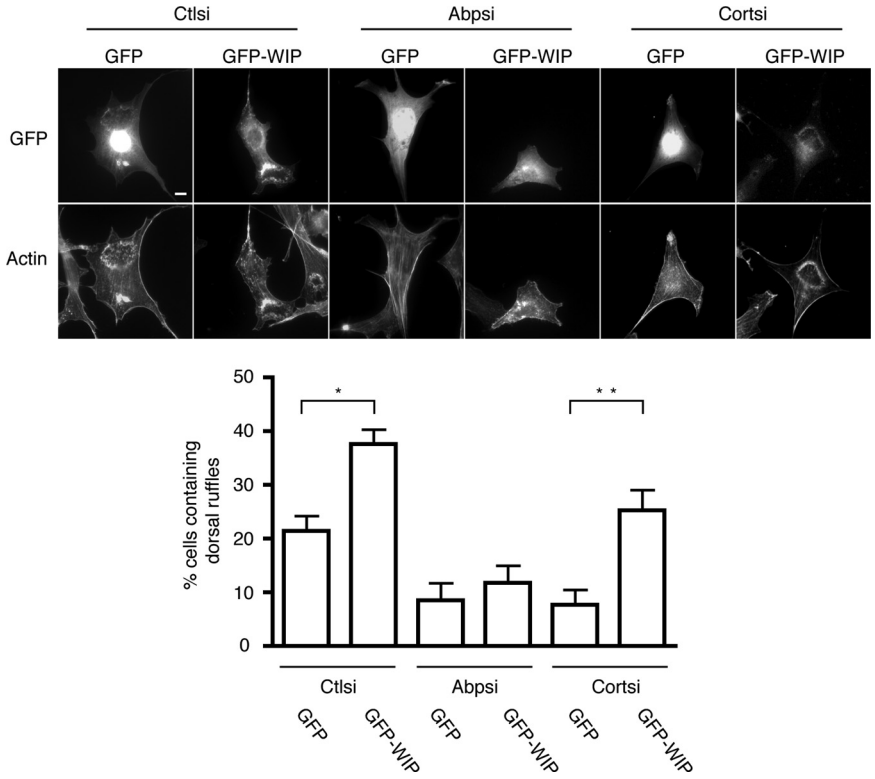

Figure 9. WIP-mediated effects on dorsal ruffles require mAbp1. NIH-3T3 cells stably expressing control, mAbp1, or cortactin siRNA were transiently transfected with GFP or GFP-WIP. Cells were plated on FN-coated coverslips, serum-starved, and stimulated with PDGF. Cells were fixed and stained with rhodamine phalloidin. Bar, 10 μm. Dorsal ruffles were quantified by counting the number of GFP-positive cells containing at least one dorsal ruffle after stimulation with PDGF. Greater than 50 cells were counted per condition, and each condition represents the average value from three independent experiments; error bars, SEM; *$p < 0.05$, compared with Ctlsi GFP, **$p < 0.01$ compared with Cortsi GFP.

is not likely to occur through its interaction with N-WASP because WIP binding to N-WASP has been shown to inhibit Arp 2/3 activity (Martinez-Quiles *et al.*, 2001). Alternatively, WIP may promote actin polymerization by its ability to stabilize F-actin (Martinez-Quiles *et al.*, 2001). In agreement with this hypothesis, the ability of WIP to regulate dorsal ruffles was shown to be dependent in part on its ability to bind actin; however, WIP regulation may also require interactions with SH3-domain–containing proteins (Anton *et al.*, 2003).

We have identified a novel, direct interaction between mAbp1 and WIP that is abrogated by a mutation in the SH3 domain of mAbp1, W415K. The SH3 domain mutant mAbp1, W415K, was unable to rescue dorsal ruffle formation in mAbp1-deficient cells, indicating that WIP binding to the SH3 domain of mAbp1 is likely critical for dorsal ruffle formation. mAbp1 binds to several proteins through its SH3 domain, and we cannot rule out that other mAbp1-binding proteins, such as dynamin, may also contribute to the regulation of dorsal ruffles by mAbp1. A mutant form of WIP, Δ110-170, which is deficient in mAbp1 binding, further supports a role for a mAbp1-WIP interaction in the formation of dorsal ruffles. In agreement with previous studies (Anton *et al.*, 2003), overexpression of wild-type WIP enhanced dorsal ruffle formation; however, the Δ110-170 WIP mutant was unable to enhance dorsal ruffle formation (Figure 8C). In further support of an important role for the WIP-mAbp1 interaction, WIP effects on dorsal ruffle formation required the expression of mAbp1 but not cortactin. The data support an essential role for mAbp1 in WIP-mediated dorsal ruffle formation. It is interesting that although PDGF treatment enhanced the interaction of mAbp1 and WIP by approximately twofold, it had no effect on the association between N-WASP and WIP (Figure 6D). Taken together, our data suggest that mAbp1 mediates dorsal ruffle formation through its interaction with WIP.

In summary, we have identified a novel role for mAbp1 in growth factor–mediated dorsal ruffle formation. Our data support a model where the mAbp1-WIP complex, independent of cortactin, is necessary for efficient dorsal ruffle formation. It is possible that mAbp1 associates with and recruits WIP to sites of growth factor–mediated actin remodeling to affect dorsal ruffle formation. However, live imaging did not provide the resolution to determine if mAbp1 is in fact recruited to dorsal ruffles before WIP. A challenge for future investigation will be to define the temporal and spatial recruitment and activity of these key actin regulatory components during the formation of dorsal ruffles. In any case, on the basis of our findings, we propose that mAbp1 recruits WIP to dorsal ruffles providing a link between the actin cytoskeleton and the Arp2/3 complex to regulate actin dynamics during dorsal ruffle formation.

ACKNOWLEDGMENTS

We acknowledge funding by the National Institutes of Health Grant R01 CA085862-08 to A.H. and by the Department of Defense predoctoral fellowship BC073295 to C.C.

REFERENCES

Anton, I. M., Jones, G. E., Wandosell, F., Geha, R., and Ramesh, N. (2007). WASP-interacting protein (WIP): working in polymerisation and much more. Trends Cell Biol. *17*, 555–562.

Anton, I. M., Saville, S. P., Byrne, M. J., Curcio, C., Ramesh, N., Hartwig, J. H., and Geha, R. S. (2003). WIP participates in actin reorganization and ruffle formation induced by PDGF. J. Cell Sci. *116*, 2443–2451.

Connert, S., Wienand, S., Thiel, C., Krikunova, M., Glyvuk, N., Tsytsyura, Y., Hilfiker-Kleiner, D., Bartsch, J. W., Klingauf, J., and Wienands, J. (2006). SH3P7/mAbp1 deficiency leads to tissue and behavioral abnormalities and impaired vesicle transport. EMBO J. *25*, 1611–1622.

Cortesio, C. L., Chan, K. T., Perrin, B. J., Burton, N. O., Zhang, S., Zhang, Z. Y., and Huttenlocher, A. (2008). Calpain 2 and PTP1B function in a novel path-

way with Src to regulate invadopodia dynamics and breast cancer cell invasion. J. Cell Biol. *180*, 957–971.

Cortesio, C. L., and Jiang, W. (2006). Mannan-binding lectin-associated serine protease 3 cleaves synthetic peptides and insulin-like growth factor-binding protein 5. Arch. Biochem. Biophys. *449*, 164–170.

Evans, J. S., and Turner, M. D. (2007). Emerging functions of the calpain superfamily of cysteine proteases in neuroendocrine secretory pathways. J. Neurochem. *103*, 849–859.

Fenster, S. D., Kessels, M. M., Qualmann, B., Chung, W. J., Nash, J., Gundelfinger, E. D., and Garner, C. C. (2003). Interactions between Piccolo and the actin/dynamin-binding protein Abp1 link vesicle endocytosis to presynaptic active zones. J. Biol. Chem. *278*, 20268–20277.

Franco, S., Perrin, B., and Huttenlocher, A. (2004). Isoform specific function of calpain 2 in regulating membrane protrusion. Exp. Cell Res. *299*, 179–187.

Han, J., Shui, J. W., Zhang, X., Zheng, B., Han, S., and Tan, T. H. (2005). HIP-55 is important for T-cell proliferation, cytokine production, and immune responses. Mol. Cell. Biol. *25*, 6869–6878.

Hou, P., Estrada, L., Kinley, A. W., Parsons, J. T., Vojtek, A. B., and Gorski, J. L. (2003). Fgd1, the Cdc42 GEF responsible for Faciogenital Dysplasia, directly interacts with cortactin and mAbp1 to modulate cell shape. Hum. Mol. Genet *12*, 1981–1993.

Huang, C., Tandon, N. N., Greco, N. J., Ni, Y., Wang, T., and Zhan, X. (1997). Proteolysis of platelet cortactin by calpain. J. Biol. Chem. *272*, 19248–19252.

Kessels, M. M., Engqvist-Goldstein, A. E., and Drubin, D. G. (2000). Association of mouse actin-binding protein 1 (mAbp1/SH3P7), an Src kinase target, with dynamic regions of the cortical actin cytoskeleton in response to Rac1 activation. Mol. Biol. Cell *11*, 393–412.

Kessels, M. M., Engqvist-Goldstein, A. E., Drubin, D. G., and Qualmann, B. (2001). Mammalian Abp1, a signal-responsive F-actin-binding protein, links the actin cytoskeleton to endocytosis via the GTPase dynamin. J. Cell Biol. *153*, 351–366.

Kinley, A. W., Weed, S. A., Weaver, A. M., Karginov, A. V., Bissonette, E., Cooper, J. A., and Parsons, J. T. (2003). Cortactin interacts with WIP in regulating Arp2/3 activation and membrane protrusion. Curr. Biol. *13*, 384–393.

Krueger, E. W., Orth, J. D., Cao, H., and McNiven, M. A. (2003). A dynamin-cortactin-Arp2/3 complex mediates actin reorganization in growth factor-stimulated cells. Mol. Biol. Cell *14*, 1085–1096.

Larbolette, O., Wollscheid, B., Schweikert, J., Nielsen, P. J., and Wienands, J. (1999). SH3P7 is a cytoskeleton adapter protein and is coupled to signal transduction from lymphocyte antigen receptors. Mol. Cell. Biol. *19*, 1539–1546.

Le Bras, S., Foucault, I., Foussat, A., Brignone, C., Acuto, O., and Deckert, M. (2004). Recruitment of the actin-binding protein HIP-55 to the immunological synapse regulates T cell receptor signaling and endocytosis. J. Biol. Chem. *279*, 15550–15560.

Legg, J. A., Bompard, G., Dawson, J., Morris, H. L., Andrew, N., Cooper, L., Johnston, S. A., Tramountanis, G., and Machesky, L. M. (2007). N-WASP involvement in dorsal ruffle formation in mouse embryonic fibroblasts. Mol. Biol. Cell *18*, 678–687.

Lokuta, M. A., Senetar, M. A., Bennin, D. A., Nuzzi, P. A., Chan, K. T., Ott, V. L., and Huttenlocher, A. (2007). Type Igamma PIP kinase is a novel uropod component that regulates rear retraction during neutrophil chemotaxis. Mol. Biol. Cell *18*, 5069–5080.

Martinez-Quiles, N., *et al.* (2001). WIP regulates N-WASP-mediated actin polymerization and filopodium formation. Nat. Cell Biol *3*, 484–491.

Mellstrom, K., Heldin, C. H., and Westermark, B. (1988). Induction of circular membrane ruffling on human fibroblasts by platelet-derived growth factor. Exp. Cell Res. *177*, 347–359.

Mise-Omata, S., Montagne, B., Deckert, M., Wienands, J., and Acuto, O. (2003). Mammalian actin binding protein 1 is essential for endocytosis but not lamellipodia formation: functional analysis by RNA interference. Biochem. Biophys. Res. Commun. *301*, 704–710.

Oda, A., *et al.* (2005). WAVE/Scars in platelets. Blood *105*, 3141–3148.

Onabajo, O. O., Seeley, M. K., Kale, A., Qualmann, B., Kessels, M., Han, J., Tan, T. H., and Song, W. (2008). Actin-binding protein 1 regulates B cell receptor-mediated antigen processing and presentation in response to B cell receptor activation. J. Immunol. *180*, 6685–6695.

Orth, J. D., Krueger, E. W., Weller, S. G., and McNiven, M. A. (2006). A novel endocytic mechanism of epidermal growth factor receptor sequestration and internalization. Cancer Res. *66*, 3603–3610.

Orth, J. D., and McNiven, M. A. (2006). Get off my back! Rapid receptor internalization through circular dorsal ruffles. Cancer Res. *66*, 11094–11096.

Perrin, B. J., Amann, K. J., and Huttenlocher, A. (2006). Proteolysis of cortactin by calpain regulates membrane protrusion during cell migration. Mol. Biol. Cell *17*, 239–250.

Ruoslahti, E., Hayman, E. G., Pierschbacher, M., and Engvall, E. (1982). Fibronectin: purification, immunochemical properties, and biological activities. Methods Enzymol *82*(Pt A), 803–831.

Schafer, D. A. (2002). Coupling actin dynamics and membrane dynamics during endocytosis. Curr. Opin. Cell Biol. *14*, 76–81.

Schafer, D. A., Weed, S. A., Binns, D., Karginov, A. V., Parsons, J. T., and Cooper, J. A. (2002). Dynamin2 and cortactin regulate actin assembly and filament organization. Curr. Biol. *12*, 1852–1857.

Schymeinsky, J., *et al.* (2009). A fundamental role of mAbp1 in neutrophils: impact on {beta}2 integrin-mediated phagocytosis and adhesion in vivo. Blood.

Suetsugu, S., Yamazaki, D., Kurisu, S., and Takenawa, T. (2003). Differential roles of WAVE1 and WAVE2 in dorsal and peripheral ruffle formation for fibroblast cell migration. Dev. Cell *5*, 595–609.

Tompa, P., Buzder-Lantos, P., Tantos, A., Farkas, A., Szilagyi, A., Banoczi, Z., Hudecz, F., and Friedrich, P. (2004). On the sequential determinants of calpain cleavage. J. Biol. Chem. *279*, 20775–20785.

Veracini, L., Franco, M., Boureux, A., Simon, V., Roche, S., and Benistant, C. (2006). Two distinct pools of Src family tyrosine kinases regulate PDGF-induced DNA synthesis and actin dorsal ruffles. J. Cell Sci. *119*, 2921–2934.

Warn, R., Brown, D., Dowrick, P., Prescott, A., and Warn, A. (1993). Cytoskeletal changes associated with cell motility. Symp. Soc. Exp. Biol. *47*, 325–338.

Wu, H., and Parsons, J. T. (1993). Cortactin, an 80/85-kilodalton pp60src substrate, is a filamentous actin-binding protein enriched in the cell cortex. J. Cell Biol. *120*, 1417–1426.